Journal of Coordination Chemistry

ISSN: (Print) (Online) Journal homepage: www.tandfonline.com/journals/gcoo20

# Kinetics and mechanistic investigation of the substitution from dinuclear Pt(II) complexes bridged by *N,N'-bis*(2-pyridylcarboxamide)phenylenediamines

Tshephiso Papo, Deogratius Jaganyi & Allen Mambanda

**To cite this article:** Tshephiso Papo, Deogratius Jaganyi & Allen Mambanda (2024) Kinetics and mechanistic investigation of the substitution from dinuclear Pt(II) complexes bridged by *N,N'-bis*(2-pyridylcarboxamide)phenylenediamines, Journal of Coordination Chemistry, 77:7-8, 638-652, DOI: 10.1080/00958972.2023.2299962

**To link to this article:** https://doi.org/10.1080/00958972.2023.2299962

JOURNAL OF COORDINATION CHEMISTRY
2024, VOL. 77, NOS. 7–8, 638–652
https://doi.org/10.1080/00958972.2023.2299962

Taylor & Francis
Taylor & Francis Group



# Kinetics and mechanistic investigation of the substitution from dinuclear Pt(II) complexes bridged by *N,N′-bis* (2-pyridylcarboxamide)phenylenediamines

Tshephiso Papo[a], Deogratius Jaganyi[b,c] and Allen Mambanda[a]

[a]School of Chemistry and Physics, University of KwaZulu-Natal, Scottsville, Pietermaritzburg, South Africa; [b]School of Pure and Applied Sciences, Mount Kenya University, Thika, Kenya; [c]Department of Chemistry, Faculty of Applied Sciences, Durban University of Technology, Durban, South Africa

**ABSTRACT**

The rates of substitution of the chloride ligand in dinuclear complexes, [$Pt_2$(*N,N′-bis*(2-pyridylcarboxamide)-1,3-phenylenediamine) $Cl_4$] (**1**), [$Pt_2$(*N,N′-bis*(2-pyridylcarboxamide)-1,4-phenylenediamine) $Cl_4$] (**2**), [$Pt_2$(*N,N′-bis*(3-isoquinolylcarboxamide)-1,3-phenylenediamine) $Cl_4$] (**3**) and [$Pt_2$(*N,N′-bis*(3-isoquinolylcarboxamide)-1,4-phenylenediamine)$Cl_4$] (**4**), by three bio-relevant nucleophiles, thiourea (TU), *N,N*-dimethylthiourea (DMTU) and *N,N,N′,N′*-tetramethylthiourea (TMTU), were investigated. The mononuclear analogue [Pt(*N*-phenylpyridine-2-carboxamide)$Cl_2$] (**5**) was included to compare the results. The kinetics of the reactions were studied under *pseudo* first-order conditions in a methanol solution ($I = 0.1$ M LiCl) as a function of concentration and temperature using the stopped-flow spectrophotometer. The observed *pseudo* first-order rate constants for the substitution reactions of all the complexes were calculated from two well-separated steps and obey the rate law $k_{obs\ (1^{st}/2^{nd})} = k_{2\ (1^{st}/2^{nd})}$[Nu]. The reactivity of the complexes decreases in the order **2** > **1** > **4** > **3** > **5**. The conformational symmetry of the complexes as controlled by the phenylenediamine bridges, steric hindrance due to the bridges as well as the σ-donor capacity of the coordinated groups around the metal centers influence the reactivity of the dinuclear complexes. The low enthalpy ($\Delta H^{\#}$) and negative intrinsic entropy ($\Delta S^{\#}$) values support an associative mechanism of substitution. The kinetic data are supported by DFT calculations.

**ARTICLE HISTORY**
Received 31 August 2023
Accepted 16 October 2023

**KEYWORDS**
Platinum complexes; carboxamide; substitution reactions; mechanistic

**CONTACT** Tshephiso Papo papot@ukzn.ac.za School of Chemistry and Physics, University of KwaZulu-Natal, Private Bag X01, Scottsville, Pietermaritzburg, 3209, South Africa

Supplemental data for this article can be accessed online at https://doi.org/10.1080/00958972.2023.2299962.

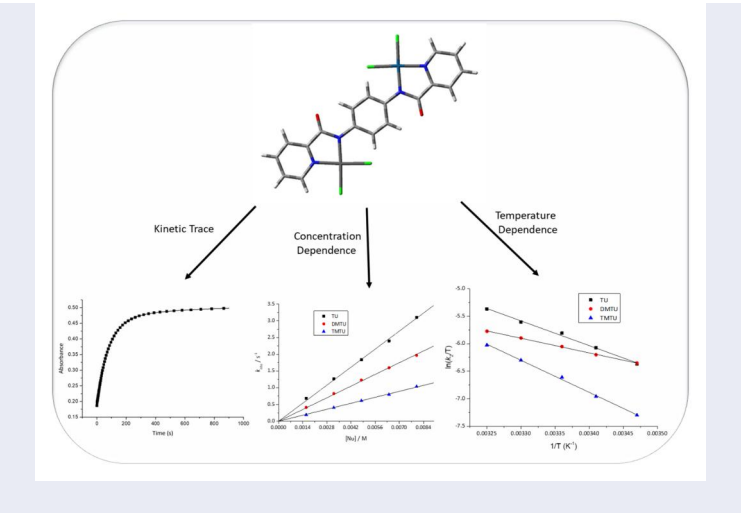


## Introduction

Covalent binding of Pt(II) and intercalation of the aromatic ligands of Pt(II) complexes to cellular DNA are the main molecular interactions associated with the activity of *cis*-Pt(II) anticancer drugs [1–4]. The tertiary structure of DNA is altered, and this results in the death of the cancer cells by apoptosis [5]. The major product of the covalent interaction of *cis*-Pt(II) anticancer agents with DNA is a 1,2-intrastrand cross-link, which makes a kink on the DNA double helix [6]. Tolerance to structural changes by cellular maintenance pathways can result in the development of cell resistance to the drug [7]. Because of this, there has been a drive to develop non-classical Pt(II) drugs [8, 9].

Researchers have moved their focus to multinuclear Pt(II) complexes that consist of two or more Pt centers linked through a bridging ligand [10–13]. Pt(II) complexes that incorporate flexible aliphatic diamine chains [14–20] or rigid aromatic [9, 12, 21–27] bridging ligands have been synthesized and tested for anti-tumor activities. Some of these complexes exhibited enhanced cytotoxicity compared to their mononuclear Pt(II) complexes partly due to the difference in the manner through which they bind to DNA [28]. The bridging ligands (linkers) of multinuclear Pt(II) complexes allow for formation of long-range intra- and inter-strand Pt-DNA crosslinks that circumvent cellular maintenance pathways linked to the development of cross-resistance to *cis*-Pt drugs [29, 30]. Another advantage is that some of the complexes have a high positive charge, which facilitates strong electrostatic interactions with DNA [29–31] to form different DNA-bound adducts. The numerous possible binding modes of the complexes to DNA enhance their biochemical activity and averts cross-resistance to classical *cis*-Pt drugs [32, 33].

Extensive work on the binding modes of dinuclear Pt(II) complexes to DNA has been conducted [28–30]. However, some physiological bionucleophiles especially proteins containing sulfur residues can potentially deactivate the Pt(II) complexes through nucleophilic substitution reactions [34]. Since Pt(II) complexes exhibit a high substitutional affinity for sulfur donor sites [34], the reactivity and thermodynamic properties

of dinuclear Pt(II) complexes bearing different chelate ligands by sulfur-containing nucleophiles have been reported. The rate of substitution from *bis*-(2-pyridylmethyl)-amine-chelated dinuclear Pt(II) complexes bridged by linkers of different flexibility [35–37] and rigidity [38] has been studied. The data suggest that the reactivity of the complexes depends on the relative σ-inductive effects, the rigidity, planarity and flexibility of the diamine linkers which induces steric influences. The reactivity of dinuclear Pt(II) complexes with bridging azines (pyrazine, 2,3-dimethylpyrazine, 2,5-dimethylpyrazine and 2,6-dimethylpyrazine), 4,4′-bipyridine and 1,2-*bis*(4-pyridyl)ethane that are *cis* [39–41] or *trans* [42, 43] to the leaving group has also been explored. The reactivity of both classes of complexes depends on the distance between the two Pt(II) centers [43], the σ-donor capacity, steric factors [40, 42] and the extent of π conjugation [41] of the bridging ligands. The substitution reactions of dinuclear Pt(II) complexes with symmetrical di(2-pyridyl)amine head groups bearing alkyl-phenyl [44] or pyridyl bridging ligands have also been studied. Their reactivity is influenced by steric effects that arise due to the bridging linker.

The reactivity and thermodynamic properties of dinuclear Pt(II) complexes with bidentate ligands bearing rigid linkers have not been explored as extensively as dinuclear Pt(II) complexes with tridentate ligands. Therefore, this work was aimed at highlighting the effect on the rate of substitution by rigid phenylenediamine bridges of dinuclear Pt(II) complexes bearing a bidentate pyridine-carboxamide or isoquinoline-carboxamide chelate group. The symmetrical [-(RN)Pt(Cl)$_2$] headgroups for these dinuclear complexes are bridged by 1,3-phenyldiamine (**1** and **2**) and 1,4-phenyldiamine (**3** and **4**) linkers. Included for comparative purposes is the mononuclear complex (**5**) which has a phenyl pendant [45]. The structures of these complexes are shown in Figure 1.

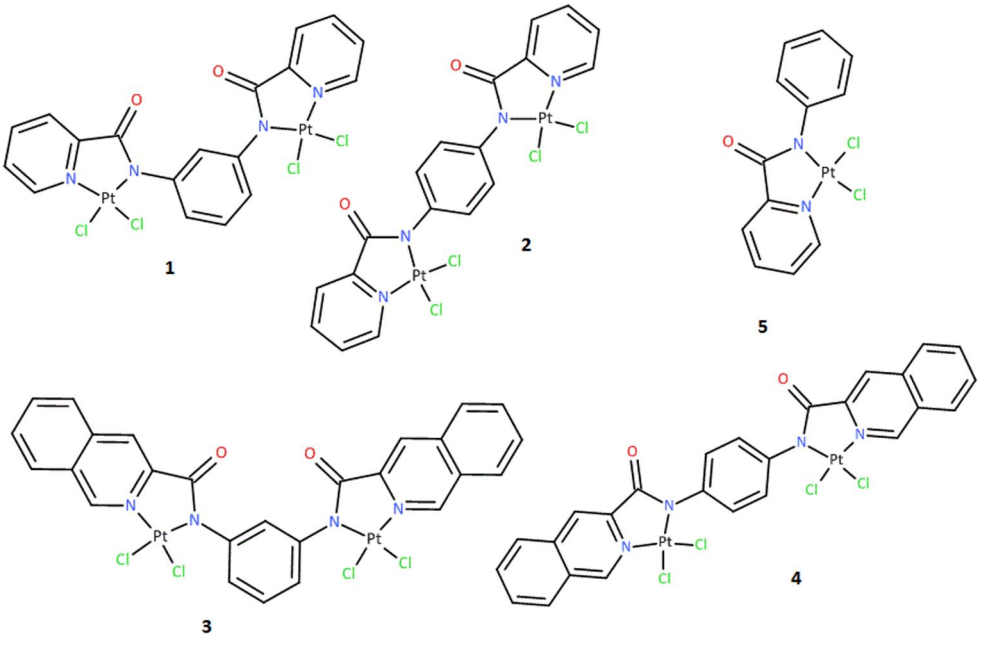


**Figure 1.** Structures of the Pt(II) complexes used in the study.

## Experimental

### Materials and reagents

The nucleophiles, thiourea (TU, 99%), *N,N*-dimethylthiourea (DMTU, 99%) and *N,N,N′,N′*-tetramethylthiourea (TMTU, 98%) and the diamine linkers aniline (99.5%), *m*-phenyldiamine (99%) and *p*-phenyldiamine (99%) were purchased from Sigma-Aldrich and used without purification. 2-Picolinic acid (99%), 3-isoquinolinecarboxylic acid hydrate (99%), triphenylphosphite (97%) and *cis*-dichlorobis(dimethyl sulfoxide)platinum(II) ($Pt(DMSO)_2Cl_2$, 97%) were also obtained from Sigma-Aldrich. All solvents (pyridine, diethyl ether and ethanol) were purchased from Merck South Africa and were of analytical grade. Methanol was Chromosolve HPLC-grade solvent. Ultrapure deionized water (Modulab systems) was used.

### Synthesis of ligands

#### *N,N′-bis(2-pyridylcarboxamide)-1,3-phenylenediamine and N,N′-bis(2-pyridylcarboxamide)-1,4-phenylenediamine*

All the ligands were synthesized according to modified literature methods [46, 47]. To a solution of picolinic acid (1.23 g, $1.00 \times 10^{-2}$ mol) or 3-isoquinoline carboxylic acid (1.73 g, $1.00 \times 10^{-2}$ mol) in pyridine (10 mL) was added a pyridine solution (5 mL) of corresponding diamine linker, *m*-phenyldiamine (0.541 g, $5.00 \times 10^{-3}$ mol) or *p*-phenyldiamine (0.541 g, $5.00 \times 10^{-3}$ mol). The mixture was stirred for 5 min at 110 °C prior to the dropwise addition of triphenylphosphite (3.102 g, $1.00 \times 10^{-2}$ mol). The solution remained colorless and was stirred for 4 h under reflux. The solution was allowed to cool to room temperature. A white precipitate was formed when distilled (10 mL) water was added to the reaction mixture. It was isolated by filtration and washed with ethanol and diethyl ether before drying under vacuum. The characterization data for the ligands is available in the Supporting Information.

### Synthesis of Pt(II) complexes

Complexes [$Pt_2$(*N,N′-bis*(2-pyridylcarboxamide)-1,3-phenylenediamine)$Cl_4$] (**1**), [$Pt_2$(*N,N′-bis*(2-pyridylcarboxamide)-1,4-phenylenediamine)$Cl_4$] (**2**), [$Pt_2$(*N,N′-bis*(3-isoquinolylcarboxamide)-1,3-phenylenediamine)$Cl_4$] (**3**) and [$Pt_2$(*N,N′-bis*(3-isoquinolylcarboxamide)-1,4-phenylenediamine)$Cl_4$] (**4**) were synthesized following the general procedure of Rauterkus *et al.* [48]. To a solution of *cis*-dichloro*bis*(dimethylsulfoxido)platinum(II), $Pt(DMSO)_2Cl_2$ (0.169 g, 0.40 mmol) in 15 mL ultra-pure water, a solution of 0.20 mmol of the corresponding bridging ligand, in 10 mL chloroform was added dropwise. The solution was refluxed for 24 h under a nitrogen atmosphere. After cooling to room temperature, the precipitate was isolated by filtration and washed with ultra-pure water (10 mL), methanol (10 mL) and diethyl ether (10 mL). All complexes were isolated in moderate yields as yellow powders and characterized using NMR ($^{1}H$,$^{13}C$,$^{195}Pt$), LC-MS spectrometry and elemental analysis. Figures S7–S12 (Supporting Information) show selected spectra.

**1**: Yield: 68%. $^{1}$H NMR (400 MHz, $CDCl_3$, 303.15 K) [δ, ppm]: 8.72 (d, 2H); 8.40 (d, 1H); 8.34 (t, 2H); 8.01 (t, 2H), 7.721 (dd, 2H); 7.59 (ddd, 2H); 7.48 (t, 1H). $^{13}$C NMR (100 MHz $CDCl_3$, 303.15 K) [δ, ppm]: 163.3, 151.1, 149.4, 138.3, 137.5, 135.5, 124.4, 123.5, 120.1, 104.4. $^{195}$Pt NMR (100 MHz; $CDCl_3$, 303.15 K) [δ, ppm]: −2398.14. TOF MS ESI$^{+}$: *m/z* 871.312 (calculated *m/z* 848.296), [(M + Na)$^{+}$]. Anal. % Calculated for $C_{18}H_{12}Cl_4N_4O_2Pt_2$: C: 25.48, H: 1.43, N: 6.60. Found: C: 25.49, H: 1.42, N: 6.58.

**2**: Yield: 61%. $^{1}$H NMR (400 MHz, DMSO-$d_6$, 303.15 K) [δ, ppm]: 9.03 (s, 2H); 8.52 (s, 2H); 8.18 (d, 2H); 8.08 (d, 2H); 7.86 (t, 2H); 7.74 (t, 2H). $^{13}$C NMR (100 MHz, DMSO-$d_6$, 303.15 K) [δ, ppm]: 163.3, 151.7, 149.4, 139.5, 138.3, 124.4, 123.5, 120.3. $^{195}$Pt NMR (100 MHz; DMSO-$d_6$, 303.15 K) [δ, ppm]: −2410.65. TOF MS ESI$^{+}$: *m/z* 871.305 (calculated *m/z* 848.296), [(M + Na)$^{+}$]. Anal. % Calculated for $C_{18}H_{12}Cl_4N_4O_2Pt_2$: C: 25.48, H: 1.43, N: 6.60. Found: C: 25.41, H: 1.45, N: 6.56.

**3**: Yield: 51%. $^{1}$H NMR (400 MHz, DMSO-$d_6$, 303.15 K) [δ, ppm]: 9.42 (s, 2H); 8.56 (s, 2H); 8.31 (d, 2H); 8.19 (d, 2H); 7.98 (t, 1H); 7.82 (t, 2H); 7.88 (t, 2H); 7.63 (dd, 2H); 7.41 (t, 1H). $^{13}$C NMR (100 MHz, DMSO-$d_6$, 303.15 K) [δ, ppm]: 164.3, 153.1, 149.6, 138.5, 135.6, 134.8, 130.4, 129.0, 128.5, 127.5, 124.2, 119.8, 117.6, 104.3. $^{195}$Pt NMR (100 MHz; DMSO-$d_6$, 303.15 K) [δ, ppm]: −2482.41. TOF MS ESI$^{+}$: *m/z* 947.13 (calculated *m/z* 947.413). Anal. % Calculated for $C_{26}H_{16}Cl_4N_4O_2Pt_2$: C: 32.92, H: 1.70, N: 5.90. Found: C: 32.94, H: 1.74, N: 5.91.

**4**: Yield: 46%. $^{1}$H NMR (400 MHz, DMSO-$d_6$, 303.15 K) [δ, ppm]: 9.51 (s, 2H); 8.53 (s, 2H); 8.36 (d, 2H); 8.26 (d, 2H); 7.88 (t, 2H); 7.72 (t, 2H); 7.39 (ddd, 4H). $^{13}$C NMR (100 MHz, DMSO-$d_6$, 303.15 K) [δ, ppm]: 163.4, 154.1, 149.6, 138.5, 136.2, 130.4, 128.8, 128.1, 127.4, 126.6, 120.3, 117.6. $^{195}$Pt NMR (100 MHz; DMSO-$d_6$, 303.15 K) [δ, ppm]: −2498.22. TOF MS ESI$^{+}$: *m/z* 972.17 (calculated *m/z* 947), [(M + Na)$^{+}$]. Anal. % Calculated for $C_{26}H_{16}Cl_4N_4O_2Pt_2$: C: 32.92, H: 1.70, N: 5.90. Found: C: 32.96, H: 1.73, N: 5.92.

## Instrumentation and physical measurements

The $^{1}$H, $^{13}$C and $^{195}$Pt NMR spectroscopic data were recorded on a Bruker Avance III 400 or a Bruker Avance III 500 spectrometer using either a 5 mm BBOZ probe or a 5 mm TBIZ probe set at 303.15 K. All recorded chemical shifts (for protons and carbons) were referenced to the signals of relevant deuterated solvents. The mass spectrometric data of the ligands and platinum complexes were obtained on a Waters Micromass LCT Premier mass spectrometer or Shimadzu LC-MS-2020. Elemental compositions for the Pt(II) complexes were obtained on a Thermo Scientific Flash 2000. The wavelengths for kinetic measurements were determined on a Varian Cary 100 Bio UV-Visible spectrophotometer. Kinetic measurements were carried out on an Applied Photophysics SX.18 MV (v4.33) stopped-flow spectrophotometer coupled to an online data acquisition system. The temperature was controlled throughout the kinetic experiments to within ± 0.1 °C using a coupled water circulating temperature control unit. All data were analyzed using the Origin 9.1® graphical analysis software package.

## Computational details

Density functional theory (DFT) calculations were performed in the gaseous state using an approach for the third-row transition metal complexes to identify the energy-minimized

structures based on the B3LYP/LANL2DZ (Los Alamos National Laboratory 2 double ξ) level theory. The singlet states were used due to the low electronic spin of Pt(II) complexes. The DFT calculations were performed using the Gaussian 09 program suite [49].

### Preparation of Pt(II) complexes and nucleophiles for kinetic measurements

The *chloro* salts of the complexes were first dissolved in 500 μL of 2% DMF solution to ensure complete dissolution. The solutions were further diluted to a final volume with 98% methanol solution with ionic strength of 0.1 M (LiCl). LiCl was added to prevent the possibility of chloride solvolysis during the substitution reactions. The nucleophiles (TU, DMTU and TMTU) were prepared fresh before use by dissolving in 0.1 M methanolic solution. The lowest concentration of the nucleophile used was at least 40-fold of the Pt(II) complex. This was done to maintain the *pseudo* first-order reaction conditions.

## Results

### Synthesis of Pt(II) complexes

The syntheses of *N,N′-bis*(2-pyridylcarboxamide)-1,3-phenylenediamine, *N,N′-bis*(2-pyridylcarboxamide)-1,4-phenylenediamine, *N,N′-bis*(3-isoquinolylcarboxamide)-1,3-phenylenediamine and *N,N′-bis*(3-isoquinolyl-carboxamide)-1,4-phenylenediamine were carried out following modified literature procedures [46, 47]. $^1$H NMR and LC-MS spectral data of the ligands are given in the Supporting Information. Reactions of the ligands with $Pt(DMSO)_2Cl_2$ in a 1:2 mol ratio resulted in formation of [$Pt_2$(*N,N′-bis*(2-pyridylcarboxamide)-1,3-phenylenediamine)$Cl_4$] (**1**), [$Pt_2$(*N,N′-bis*(2-pyridylcarboxamide)-1,4-phenylenediamine)$Cl_4$] (**2**), [$Pt_2$(*N,N′-bis*(3-isoquinolylcarboxamide)-1,3-phenylenediamine)$Cl_4$] (**3**) and [$Pt_2$(*N,N′-bis*(3-isoquinolylcarboxamide)-1,4-phenylenediamine)$Cl_4$] (**4**). The Pt(II) coordinates in a bidentate mode *via* the negatively charged amide and the pyridine of the ligand chelate. All Pt(II) complexes were obtained in low to good yields (46-68%). $^1$H NMR spectral data of the free ligands (Figures S1–S3 in the Supporting Information) revealed a signal of the carboxamide proton (R-C(=O)-N**H**-R) between 10.14 and 10.82 ppm. Upon complexation, the carboxamide peak was absent in the $^1$H NMR spectra of the complexes proving that the ligands have coordinated to the metal and that the N-H deprotonated upon complexation. Mass spectrometry was further used to elucidate the composition of the molecular formulas of the complexes. The data showed molecular fragmentation patterns consistent with the formation of dinuclear *bis*(-chelated) Pt(II) complexes. Elemental analyses of all the complexes were consistent with the proposed structures.

### Density functional theory calculations

Representative geometry-optimized structures for the complexes are presented in Table 1. Selected bond lengths, bond angles and natural atomic bond orbital (NBO) charges are shown in Table 2. From the bond angles around the Pt ion in Table 1, the

**Table 1.** Geometry-optimized structures and DFT-calculated HOMO and LUMO maps.

| Complex | HOMO | LUMO | Orientation |
|---|---|---|---|
| 5 |  | 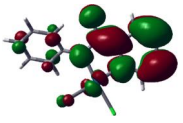 |  |
| 1 | 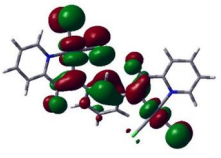 | 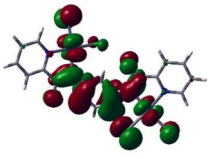 | 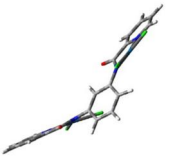 |
| 2 | 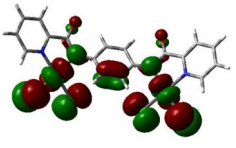 | 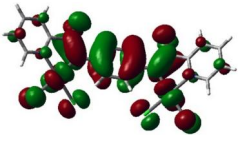 | 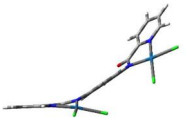 |
| 3 | 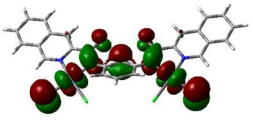 | 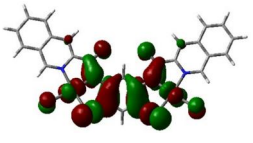 | 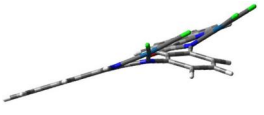 |
| 4 | 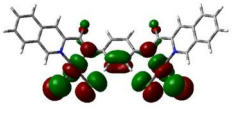 | 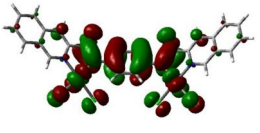 | 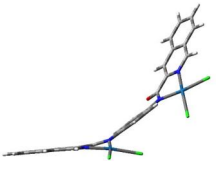 |

geometry of coordinated ligands is distorted square-planar. In general, the plane of the phenyl rings in each bridging ligand is perpendicular or at an angle to the square plane of the Pt(II) center. This also affects the strength of the bonds between Pt and the donor atoms of the bidentate chelate bridges. Weaker bonds on the non-leaving ligands lead to a poor *trans* influence on the co-ligands opposite to the donor atoms. The Pt-$Cl_1$ (*trans* to the pyridine) bond length in all complexes is longer than the Pt-$Cl_2$ (*trans* to the RNCO carboxamide group), an indication that the pyridine is a net $\pi$-accepter while the amide group is a $\sigma$-donor. The separation distance between the two Pt(II) centers is shorter for the 1,3-phenylenic (*meta*) bridge than for the 1,4-phenylenic (*para*). The highest occupied molecular orbitals (HOMO) are located mainly on the metal and the chloro groups while the lowest unoccupied molecular orbitals (LUMO) are located on the pyridine-carboxamide/3-isoquinoline-carboxamide ligands.

## *Kinetic measurements*

The rates of substitution reactions of coordinated chloride ligands from **5** and four dinuclear Pt(II) complexes (**1**, **2**, **3** and **4**) by sulfur donor nucleophiles (TU, DMTU and TMTU) were studied under *pseudo* first-order conditions. The stopped-flow

**Table 2.** Summary of DFT-calculated parameters for the Pt(II) complexes.

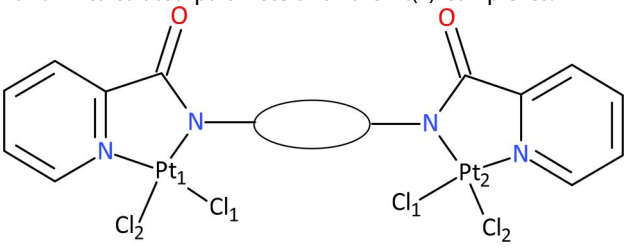


a

| Complex | 5 | 1 | 2 | 3 | 4 |
|---|---|---|---|---|---|
| Property | | | | | |
| Bond lengths (Å) | | | | | |
| $Pt_1$-$Cl_1$ | 2.394 | 2.399 | 2.392 | 2.411 | 2.393 |
| Pt-$Cl_2$ | 2.391 | 2.389 | 2.392 | 2.404 | 2.395 |
| Pt-$N_1$ | 2.055 | 2.048 | 2.042 | 2.031 | 2.041 |
| Pt-$N_2$ | 2.002 | 2.022 | 2.030 | 2.025 | 2.029 |
| Separation distance (Å) | | | | | |
| $Pt_1$ – $Pt_2$ | – | 7.776 | 7.988 | 7.781 | 7.982 |
| Bond angles (°) | | | | | |
| $N_1$-Pt-$N_2$ | 81.97 | 81.40 | 81.85 | 82.04 | 81.94 |
| Natural charges | | | | | |
| $Pt_1$ | 0.453 | 0.232 | 0.392 | 0.402 | 0.390 |
| $Pt_2$ | – | 0.235 | 0.392 | 0.402 | 0.390 |
| HOMO (eV) | −7.171 | −6.317 | −6.501 | −6.163 | −6.287 |
| LUMO (eV) | −3.497 | −5.541 | −5.242 | −5.111 | −5.042 |
| ΔE (eV) | 3.674 | 0.776 | 1.259 | 1.052 | 1.245 |
| Chemical hardness ($\eta$) | 1.8370 | 0.3880 | 0.6295 | 0.5260 | 0.6225 |
| Electrophilicity index ($\omega$) | 7.74 | 52.00 | 27.38 | 30.21 | 25.77 |

[a]A common atom numbering applies for structure data of 1–4.

spectrophotometer was used for kinetic measurements by following the change in absorbance at suitable wavelengths (Table S1) as a function of time. The time-dependent spectra observed for all reactions fit perfectly to two resolvable single exponential decay functions to generate two *pseudo* first-order rate constants, $k_{obs(1^{st}/2^{nd})}$. Thus, the substitution reaction pathway of all the complexes comprises two well-separated steps, characterized kinetically by associative rate constants, $k_{2(1^{st}/2^{nd})}$. Typical kinetic traces for the substitution steps indicating the reaction between **2** ($4.0 \times 10^{-5}$ M) and TU ($4.8 \times 10^{-3}$) at 298 K in a methanol solution ($I = 0.1$ M LiCl) are shown in Figure 2. The *pseudo* first-order rate constants, $k_{obs(1^{st}/2^{nd})}$, were calculated from the kinetic traces using the online non-linear least squares fit of exponential standard decay functions on the Stopped-Flow spectrophotometer and the data were analyzed using origin 9.1® graphical analysis software.

## *Concentration dependence*

The *pseudo* first-order rate constants, $k_{2(1^{st}/2^{nd})}$ were plotted as a function of the concentration of the thiourea nucleophiles, resulting in a linear dependence with a zero intercept. Scheme 1 depicts the generalized mechanism of substitution, shown for the reactions of **2** with the thiourea nucleophiles. Equations 1a and 1b represent the rate law for the two substitution steps.

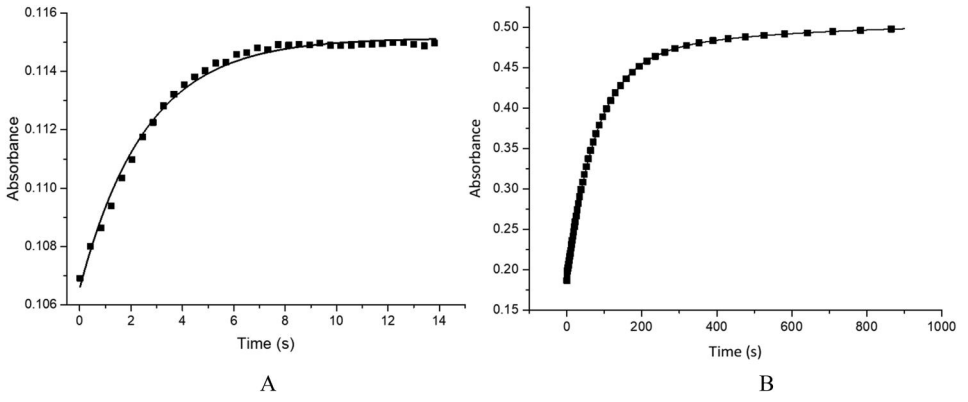


**Figure 2.** Kinetic trace obtained from the stopped-flow spectrophotometer showing a single exponential fit between the reaction of **2** ($4.0 \times 0^{-5}$ M) and TU ($4.8 \times 10^{-3}$ M) in methanol solution ($I = 0.1$ M LiCl) for the first (A) and second (B) substitution steps followed at 286 nm.

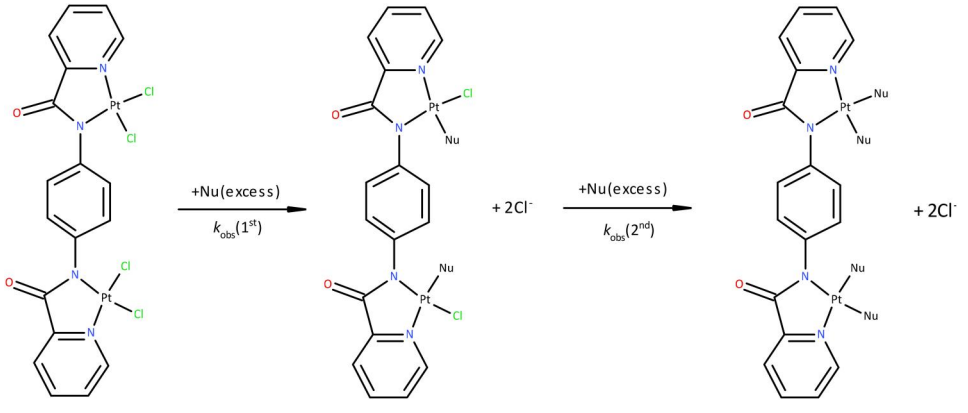


**Scheme 1.** The reaction pathway for the substitution reactions of **2** with the respective thiourea nucleophiles in methanol solution ($I = 0.1$ M LiCl).

$$k_{obs}(1^{st}) = k_2(1^{st})[Nu] \quad (1a)$$

$$k_{obs}(2^{nd}) = k_2(2^{nd})[Nu] \quad (1b)$$

Typical plots of the observed *pseudo* first-order rate constants against the concentration of nucleophiles for the first and second substitution steps are indicated in Figure 3 for **2** (for related plots of **1**, **3** and **4**, see also Figures S14-S19 in the Supporting Information). The second-order rate constants, $k_{2(1^{st}/2^{nd})}$, were obtained from the slopes of these plots and the values are summarized in Table 3.

## *Activation parameters*

The temperature dependences of the second-order rate constants ($k_{2(1^{st}/2^{nd})}$) for the two substitution steps were investigated over the temperature range of 288 K to 308 K at 5 K intervals. Representative Eyring plots for the first and second substitution steps are shown in Figure 4 for **1** (for plots of **2**, **3** and **4**, see also Figures S20–S27 in the Supporting Information). The enthalpy of activation ($\Delta H^{\#}$) and entropy of activation

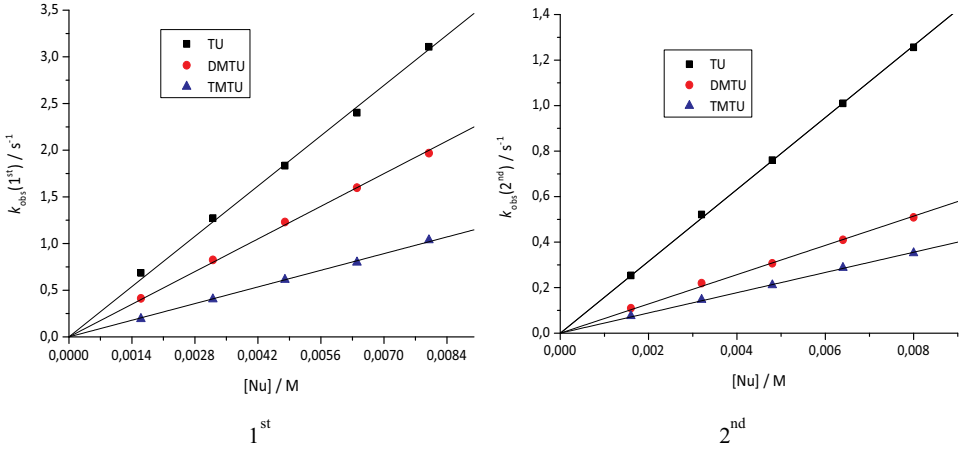


**Figure 3.** Plot of $k_{obs}$ against nucleophile concentration for the substitution of the first and second chloride ligands in **2** in methanol solution ($I = 0.1$ M LiCl) at 298 K.

**Table 3.** Summary of rate constants ($k_{2(1st/2nd)}$) for the substitution of chloride from the complexes by neutral nucleophiles in methanol solution ($I = 0.1$ M LiCl).

| Complex | Nu | $k_{2(1st)}$, $M^{-1}$ $s^{-1}$ | $k_{2(2nd)}$, $M^{-1}$ $s^{-1}$ |
|---|---|---|---|
| **5** | TU | 129 ± 1 | 26 ± 0.3 |
| | DMTU | 41 ± 0.3 | 10.00 ± 0.02 |
| | TMTU | 9.2 ± 0.2 | $1.0 \pm 0.5 \times 10^{-3}$ |
| **1** | TU | 327 ± 2 | 104 ± 1 |
| | DMTU | 192 ± 2 | 63 ± 1 |
| | TMTU | 94 ± 1 | 37 ± 1 |
| **2** | TU | 384 ± 5 | 157 ± 2 |
| | DMTU | 249 ± 2 | 76 ± 0.4 |
| | TMTU | 127 ± 1 | 56 ± 0.3 |
| **3** | TU | 158 ± 1 | 63 ± 0.3 |
| | DMTU | 64 ± 1 | 33 ± 1 |
| | TMTU | 44 ± 0.3 | 12 ± 0.3 |
| **4** | TU | 192 ± 2 | 74 ± 0.5 |
| | DMTU | 128 ± 2 | 56 ± 0.2 |
| | TMTU | 95 ± 0.3 | 26 ± 0.5 |

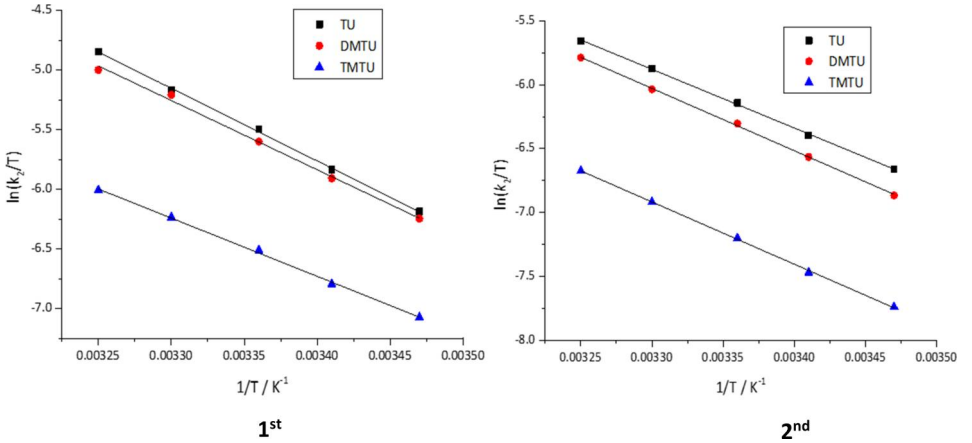


**Figure 4.** Plots of $ln\left(\frac{k2}{T}\right)$ against $\frac{1}{T}$ for the reactions of **1** with three thiourea nucleophiles in the temperature range 288 to 308 K for the first and second substitution step in 0.1 M methanol solution.

**Table 4.** Summary of activation parameters for the substitution of chloride by thiourea nucleophiles in methanol solution ($I = 0.1$ M LiCl).

| | | Activation enthalpy (kJ mol$^{-1}$) | | Activation entropy (J K$^{-1}$ mol$^{-1}$) | |
|---|---|---|---|---|---|
| Complex | Nu | $\Delta H_1$ | $\Delta H_2$ | $\Delta S_1$ | $\Delta S_2$ |
| **5** | TU | 50 ± 3 | 43 ± 4 | −105 ± 8 | −142 ± 12 |
| | DMTU | 46 ± 3 | 44 ± 4 | −129 ± 9 | −165 ± 12 |
| | TMTU | 54 ± 0.5 | 52 ± 3 | −155 ± 2 | −176 ± 8 |
| **1** | TU | 51 ± 0.8 | 46 ± 2 | −67 ± 3 | −85 ± 8 |
| | DMTU | 48 ± 2 | 41 ± 2 | −75 ± 6 | −109 ± 8 |
| | TMTU | 41 ± 1 | 42 ± 1 | −109 ± 3 | −110 ± 3 |
| **2** | TU | 46 ± 2 | 23 ± 1 | −114 ± 5 | −163 ± 3 |
| | DMTU | 44 ± 0.5 | 42 ± 0.7 | −167 ± 2 | −109 ± 3 |
| | TMTU | 49 ± 1 | 29 ± 1 | −84 ± 4 | −159 ± 3 |
| **3** | TU | 46 ± 2 | 43 ± 2 | −85 ± 5 | −156 ± 6 |
| | DMTU | 51 ± 0.6 | 36 ± 1 | −71 ± 2 | −144 ± 3 |
| | TMTU | 50 ± 1 | 40 ± 2 | −81 ± 3 | −122 ± 6 |
| **4** | TU | 45 ± 0.5 | 28 ± 1 | −156 ± 1.6 | −166 ± 3 |
| | DMTU | 38 ± 0.3 | 32 ± 1 | −179 ± 0.9 | −146 ± 3 |
| | TMTU | 67 ± 4 | 30 ± 1 | −142 ± 12 | −159 ± 3 |

($\Delta S^{\#}$) were determined from the slope and the y-intercept of the Eyring plots, respectively. The activation parameters are summarized in Table 4.

## Discussion

New dinuclear square planar *tetra*-chloro Pt(II) complexes that consist of a bidentate pyridine-carboxamide or an isoquinoline-carboxamide inert chelate were synthesized. The dinuclear Pt(II) complexes are linked by rigid phenylenediamine bridges coupled to either pyridylcarboxamide or quinolylcarboxamide coordinating chelates. Complexes **1** and **2** have a common pyridine-carboxamide head group while **3** and **4** have a similar isoquinoline-carboxamide head group. **5** is the monomer analogue of the dinuclear complexes.

The marked rigidity of the phenylenediamine bridges of **1**-**4** leads to structural and conformational differences that influence the substitutional reactivity of these complexes. The rates of substitution from these Pt(II) complexes with thiourea-based nucleophiles at different concentrations and temperatures were measured. The substitution reactions of **1**-**4** took place *via* a two-step reaction. The rate constants for the first step, $k_{2(1st)}$, represent the rates of simultaneous substitution of the respective chloride ligand *trans* to the pyridine/isoquinoline nitrogen atoms. In the second substitution step, the rate constants, $k_{2(2^{nd})}$, represent the rates of simultaneous substitution of the second chloride ligands *trans* to the amide nitrogen. The substitution pathway follows a similar trend observed for mononuclear bidentate Pt(II) complexes, where $^{195}$Pt NMR spectroscopy was used to monitor the reaction progress and confirmed that the two substitution steps were due to different rates of substitution of the chloride ligands [45]. For the dinuclear dichloro Pt(II) complexes studied herein, simultaneous chloro substitution happens irrespective of the nature of the spacer group and is consistent with the symmetrical consideration of the chelate groups in each complex. The two chloride groups *trans* to the pyridine on each Pt(II) center are substituted first due to the stronger *trans* effect of the pyridine ring relative to the amide group which

has σ-donor properties. The rate of substitution of the second chloride is more than two orders of magnitude slower than the first. The binding of the first nucleophile hinders incoming nucleophiles towards substitution. Both substitution steps are sensitive to variations in the nature of the bridging ligand and follow similar processes.

The lability of the chloride ligands depends on the nature, conformations, steric influences and the distance between the two Pt(II) centers. A comparison of the rate constants in Table 3 indicates that substitutions of the chloride ligands occur faster for the dinuclear Pt(II) complex when compared to the mononuclear analogue. This is unlike what has been reported for structurally related complexes [35, 44]. In earlier reports, the rate of substitution from the mononuclear Pt(II) analogue was much higher than the dinuclear Pt(II) complexes, attributed to the increased steric demand in dinuclear Pt(II) compared to mononuclear Pt(II) complexes. In the current study, the electronic effects play a significant role over steric influences when comparing the reactivity of the mononuclear and the dinuclear Pt(II) complexes. This is reflected in the relative magnitude of the electrophilicity index ($\omega$) indicated in Table 2, for which **5** (7.74) is the lowest compared to all the dinuclear complexes. This can be attributed to the fact that the σ-inductive effect due to phenyl is shared between two Pt(II) centers in the cases of dinuclear complexes, unlike in the case of the mononuclear complex. The chemical hardness ($\eta$) for **5** (8.8370) is the highest compared to the other complexes, making it less reactive towards the nucleophile.

Complexes **1** and **2** have a common bidentate pyridine-carboxamide chelate. The chelates are bridged by *m*-phenylenediamine linker in **1**, while in **2** they are linked by *p*-phenylenediamine. The difference in NBO charges of the Pt centers is based on the symmetry of the complexes, which controls the orbital overlaps and introduces steric effects. Complexes **1** and **2** are structural isomers. The reactivity of **2** is marginally higher than that of **1**. The DFT calculated data in Table 2 show a higher HOMO – LUMO energy gap (ΔE) and chemical hardness in **2** compared to **1**. One would therefore expect **1** to be more reactive. The electrophilicity index also supports this, but the increased reactivity of **2** is due to a slightly higher steric hindrance in **1** in comparison to **2**. This is because as the position of the phenyl group changes from *meta* to *para*, the distance between the two Pt(II) centers increases by 0.212 Å. Steric hindrance in **2** is therefore reduced, thus the substitution of chloride is faster.

The decrease in reactivity of **3** and **4** compared to the other dinuclear complexes is attributed to the relatively poor π-acceptor property of the isoquinoline ligand and the fact that the isoquinoline ligand is a net σ-donor. This causes the metal center to be less electrophilic, resulting in retardation of the incoming nucleophiles. Similar results have been reported previously [50–53] where the increase in the *cis* σ-effect caused a decrease in the rate of substitution reactions of Pt(II) complexes. In addition, steric hindrance also plays a role. The reactivity of **4** is slightly higher than that of **3**. One would have expected **3** to be more reactive than **4**, looking at the DFT calculated data in Table 1. The HOMO – LUMO energy gap for **4** is greater than the HOMO – LUMO energy gap in **3**, making **4** harder and less reactive. The electrophilicity index for **4** (25.77) is lower than that for **3** (30.21), which further supports the expected reduced reactivity in **3**. Steric influences caused by the geometric configuration of the bridging ligand of **3** influence the reactivity of the complex. Steric hindrance

influences the reactivity of the two complexes because the Pt-Pt distance in **4** (7.982 Å) is longer compared to **3** (7.781 Å), which indicates increased steric influence, and therefore slower reactivity in **3**.

The substitution of chloride ligand by thiourea nucleophiles TU, DMTU and TMTU decreases according to the increase in steric effects of the nucleophiles for all the complexes. The most sterically hindered TMTU reacts considerably slower. The positive enthalpy of activation ($\Delta H^{\#}$) and negative intrinsic entropy of activation ($\Delta S^{\#}$) values indicated in Table 4 characterize an associative mechanism of substitution well known for $d^8$ square-planar metal complexes.

## Conclusion

The study shows that the nature of the bridging phenylenediamine ligand influences the reactivity at both the metal centers in dinuclear Pt(II) complexes. The introduction of an isoquinoline moiety in the coordinating head groups of **3** and **4** retards chloro-substitution from the complexes compared to **1** and **2**. Expansion of the $\pi$ surface of the head groups of **3** and **4** does not result in increased $\pi$-back bonding due to a net $\sigma$ donor capacity of isoquinoline towards the metal centers. This reduces the electrophilicity, resulting in reduced reactivity. Changing the linking positions in the phenyl spacer from *meta* to *para* causes an increase in the Pt-Pt distance which reduces the steric influences of the bridge and thus increases the reactivity of the complexes. The substitution pathway of the studied complexes is two-steps with the second two orders of magnitude lower than the first. However, both are sensitive to the structural changes originating from the linking phenylenediamine bridge. The negative activation entropy ($\Delta S^{\#}$) supports an associative mechanism of substitution for **1**-**4**.

## Disclosure statement

No potential conflict of interest was reported by the author(s).

## Funding

The authors gratefully acknowledge financial support from the University of KwaZulu-Natal and the National Research Foundation (NRF) of South Africa.

## ORCID

Tshephiso Papo http://orcid.org/0000-0002-7860-1442

## References

[1] D. Wang, S.J. Lippard. *Nat. Rev. Drug Discov.*, **4**, 307(2005).
[2] G. Momekov, A. Bakalova, M. Karaivanova. *Curr. Med. Chem.*, **12**, 2177(2005).
[3] C.X. Zhang, S.J. Lippard. *Curr. Opin. Chem. Biol.*, **7**, 481(2003).
[4] Y. Jung, S.J. Lippard. *Chem. Rev.*, **107**, 1387(2007).
[5] T.W. Hambley. *J. Chem. Soc, Dalton Trans.*, **19**, 2711(2001).
[6] L. Fourrier, P. Brooks, J.M. Malinge. *J. Biol. Chem.*, **278**, 21267(2003).

[7] J. Reedijk. *Platinum Met. Rev*, **52**, 2(2008).
[8] N.J. Wheate, S. Walker, G.E. Craig, R. Oun. *Dalton Trans.*, **39**, 8113(2010).
[9] S. Komeda, M. Lutz, A.L. Spek, Y. Yamanaka, T. Sato, M. Chikuma, J. Reedijk. *J. Am. Chem. Soc.*, **124**, 4738(2002).
[10] N. Farrell, Y. Qu, M.P. Hacker. *J. Med. Chem.*, **33**, 2179(1990).
[11] B.A.J. Jansen, J. van Der Zwan, H. den Dulk, J. Brouwer, J. Reedijk. *J. Med. Chem.*, **44**, 245(2001).
[12] N.J. Wheate, C. Cullinane, L.K. Webster, J.G. Collins. *Anti-Cancer Drug Des*, **16**, 91(2001).
[13] N.J. Wheate, J.G. Collins. *Curr. Med. Chem. Anticancer. Agents.*, **5**, 267(2005).
[14] (a) N. Farrel, S.G. de Almeida, K.A. Skov. *J. Am. Chem. Soc.*, **110**, 5018(1988). (b) N. Farrell, Y. Qu. *Inorg. Chem.*, **28**, 3416(1989).
[15] N. Farrell. *Met. Ions Biol. Syst*, **42**, 251(2004).
[16] H. Rauter, R. Domenico, E. Menta, A. Oliva, Y. Qu, N. Farrel. *Inorg. Chem.*, **36**, 3919(1997).
[17] V. Brabec, J. Kaspárková, O. Vrána, O. Nováková, J.W. Cox, Y. Qu, N. Farrell. *Biochemistry*, **38**, 6781(1999).
[18] N. Farrell, Y. Qu, L. Feng, B. Van Houten. *Biochemistry*, **29**, 9522(1990).
[19] Y. Qu, N. Farrell. *J. Am. Chem. Soc.*, **113**, 4851(1991).
[20] J.W. Williams, Y. Qu, H.B. Genevieve, E. Alvorado, N.P. Farrell. *Inorg. Chem.*, **46**, 5820(2007).
[21] S. Komeda, G.V. Kalayda, M. Lutz, A.L. Spek, Y. Yamanaka, T. Sato, M. Chikuma, J. Reedijk. *J. Med. Chem.*, **46**, 1210(2003).
[22] S. Komeda, M. Lutz, A.L. Spek, M. Chikuma, J. Reedijk. *Inorg. Chem.*, **39**, 4230(2000).
[23] N.A. Kas'yanenko, E.E.F. Aia, A.A. Bogdanov, Y.V. Kosmotynskaya, K.I. Yakovlev. *Mol. Biol*, **36**, 745(2002).
[24] G.V. Kalayda, S. Komeda, K. Ikeda, T. Sato, M. Chikuma, J. Reedijk. *Eur. J. Inorg. Chem.*, **2003**, 4347(2003).
[25] G.V. Kalayda, B.A.J. Jansen, P. Wielaard, H.J. Tanke, J. Reedijk. *J. Biol. Inorg. Chem.*, **10**, 305(2005).
[26] A.A. Franich, M.D. Živković, T. Ilić-Tomić, I.S. Đorđević, J. Nikodinović-Runić, A. Pavić, G.V. Janjić, S. Rajković. *J. Biol. Inorg. Chem.*, **25**, 395(2020).
[27] L. Senerovic, M.D. Zivkovic, A. Veselinovic, A. Pavic, M.I. Djuran, S. Rajkovic, J. Nikodinovic-Runic. *J. Med. Chem.*, **58**, 1442(2015).
[28] J. Kasparkova, O. Vrana, N. Farrell, V. Brabec. *J. Inorg. Biochem.*, **98**, 1560(2004).
[29] A. Hegmans, S.J. Berners-Price, M.S. Davies, D.S. Thomas, A.S. Humphreys, N. Farrell. *J. Am. Chem. Soc.*, **126**, 2166(2004).
[30] R.A. Ruhayel, J.J. Moniodis, X. Yang, J. Kasparkova, V. Brabec, S.J. Berners-Price, N.P. Farrell. *Chemistry*, **15**, 9365(2009).
[31] Q. Liu, Y. Qu, R. van Antwerpen, N. Farrell. *Biochemistry*, **45**, 4248(2006).
[32] S. Komeda, Y. Qu, J.B. Mangrum, A. Hegmans, L.D. Williams, N.P. Farrell. *Inorg. Chim. Acta*, **452**, 25(2016).
[33] C. Manzotti, G. Pratesi, E. Menta, R. Di Domenico, E. Cavalletti, H.H. Fiebig, L.R. Kelland, N. Farrell, D. Polizzi, R. Supino, G. Pezzoni, F. Zunino. *Clin. Cancer Res*, **6**, 2626(2000).
[34] D.L. Bodenner, P.C. Dedon, P.C. King, R.F. Borch. *Cancer Res*, **46**, 2745(1986).
[35] (a) A. Mambanda, D. Jaganyi. *Dalton Trans*, **41**, 908(2012). (b) M. Chipangura, A. Mambanda, D. Jaganyi. *J. Coord. Chem*, **67**, 2048(2014).(c) M. Chipangura, A. Mambanda, D. Jaganyi. *Transition Met. Chem.*, **40**, 109(2015).
[36] H. Ertürk, A. Hofmann, R. Puchta, R. van Eldik. *Dalton Trans.*, **22**, 2295(2007).
[37] H. Ertürk, J. Maigut, R. Puchta, R. van Eldik. *Dalton Trans.*, **20**, 2759(2008).
[38] A. Hofmann, R. van Eldik. *Dalton Trans*, **15**, 2979(2003).
[39] P. Ongoma, D. Jaganyi. *Int. J. of Chemical Kinetics*, **45**, 676(2013).
[40] P. Ongoma, D. Jaganyi. *Dalton Trans.*, **42**, 2724(2013).
[41] P. Ongoma, D. Jaganyi. *Transition Met. Chem.*, **38**, 587(2013).
[42] D. Reddy, D. Jaganyi. *Int. J. of Chemical Kinetics*, **43**, 161(2011).
[43] T. Soldatović, S. Jovanović, ŽD. Bugarčić, R. van Eldik. *Dalton Trans.*, **41**, 876(2012).
[44] W.P. Asman, D. Jaganyi. *Int. J. Chem. Kinet.*, **49**, 545(2017).

[45] T. Papo, D. Jaganyi, A. Mambanda. *J. Coord. Chem*, **75**, 2557(2022).
[46] Z. Han, C. Lu, S. Huang, X. Chai, Z. Chen, X. Li, J. Wang, J. Zhang, B. Feng, S. Han, R. Li. *Dalton Trans.*, **52**, 16217(2002).
[47] C.R. Wilson, A.M. Fagenson, W. Ruangpradit, M.T. Muller, O.Q. Munro. *Inorg. Chem.*, **52**, 7889(2013).
[48] M.J. Rauterkus, S. Fakih, C. Mock, I. Puscasu, B. Krebs. *Inorg. Chim. Acta*, **350**, 355(2003).
[49] G.W. Trucks, M.J. Frisch, H.B. Schlegel, G.E. Scuseria, J.R. Cheeseman, M.A. Robb, G. Scalmani, V. Barone, G.A. Petersson, B. Mennucci, H. Nakatsuji, M. Caricato, X. Li, A.F. Izmaylov, H.P. Hratchian, J. Bloino, G. Zheng, M. Hada, J.L. Sonnenberg, M. Ehara, K. Toyota, R. Fukuda, M. Ishida, J. Hasegawa, T. Nakajima, Y. Honda, O. Kitao, T. Vreven, H. Nakai, J.A. Montgomery, Jr., J.E. Peralta, M. Bearpark, F. Ogliaro, J.J. Heyd, E. Brothers, K.N. Kudin, R. Kobayashi, V.N. Staroverov, J. Normand, K. Raghavachari, J.C.B.A. Rendell, S.S. Iyengar, J. Tomasi, M. Cossi, J.M.M.N. Rega, M. Klene, J.E. Knox, J.B. Cross, C. Adamo, V. Bakken, J. Jaramillo, R. Gomperts, R.E. Stratmann, O. Yazyev, A.J. Austin, R. Cammi, C. Pomelli, R.L. Martin, J.W. Ochterski, K. Morokuma, V.G. Zakrzewski, G.A. Voth, P. Salvador, J.J. Dannenberg, S. Dapprich, O. Farkas, A.D. Daniels, J.B. Foresman, J.V. Ortiz, J. Cioslowski, D.J. Fox. *Gaussian 09 (Revision A.1)*, Inc., Wallingford, CT 2009
[50] D. Jaganyi, D. Reddy, J.-A. Gertenbach, A. Hofmann, R. van Eldik. *Dalton Trans.*, **2**, 299(2004).
[51] P. Ongoma, D. Jaganyi. *Dalton Trans.*, **41**, 10724(2012).
[52] G. Kinunda, D. Jaganyi. *Transition Met. Chem.*, **39**, 451(2014).
[53] A. Topolski, P. Rozmarynowska, M. Maj, R. Czajkowski. *Inorg. Chim. Acta*, **462**, 10(2017).